Metal-oxygen Fusion: Experimental Confirmation of an Ohsawa-Kushi Transmutation and an Exploration of Low-energy Nuclear Reactions

Preprint · February 2021

DOI: 10.13140/RG.2.2.36203.05926

2 authors:

Kenneth N. Swartz
K-Orbital
7 PUBLICATIONS **0** CITATIONS
SEE PROFILE

Gary J Rodriguez
sysRAND Corporation (3.0)
51 PUBLICATIONS **9** CITATIONS
SEE PROFILE

Metal–Oxygen Fusion:
Experimental Confirmation of an Ohsawa-Kushi Transmutation and an Exploration of Low-Energy Nuclear Reactions

Kenneth N. Swartz

Abstract

There have been numerous low-energy nuclear reaction (LENR) experiments that produce results suggestive of nuclear fusion. These experiments stretch back from the early 1900s to the present. Significant excess amounts of heat are emitted from these reactions—greater than their electrical and chemical energy inputs. Most of these LENRs, or "new hydrogen energy" experiments, are based on electrolytic or electrical discharge plasma reactors. Results suggestive of fusion include the detection of gamma- and X-ray radiation; alpha, beta, neutron, and proton emissions; as well as helium-4. X-ray spectroscopic analysis of the metal electrodes used in LENR experiments has resulted in the discovery of new elements not originally present in the electrode metal. There are no currently accepted fusion synthesis pathways to account for the appearance of these new elements. Metal–oxygen fusion (MOXY) can explain many LENR results. At the nanoscale level, MOXY is more characteristic of fusion occurring within the degenerate matter of stellar cores. As a process, MOXY can be classified as a form of hot fusion. MOXY can help explain the fusion synthesis and decay pathways observed in LENRs. The MOXY process appears to have a greater propensity to occur when using elements with greater atomic weight, as well as with heavier isotopes of elements. Significant reductions in heavy radioactive nucleotides are observed with MOXY fusion.

Introduction

Controversy exists on the subject of low-energy nuclear reaction (LENR) experimental claims. Some researchers who conducted these experiments and allege the result of fusion have not been able to reproduce the reactions consistently. Many LENR experiments produce intermittent, small, or potentially debatable fusion signatures, as shown in the work of Krivit (2005) and Swartz (2009).

Nearly all research on LENR experiments focuses almost exclusively on various isotopes of hydrogen or helium-3 (^{3}He)/deuterium–based fusion. LENR fusion can occur in the absence of deuterium or hydrogen, as long as both oxygen and a metal are present. Deuterium may be a source of neutron emissions in some LENRs.

Another problem common to LENR experiments is the absence of accepted fusion pathways to explain the generation of new elements. This situation has rendered the case for LENRs murky and evocative of pseudoscience. The metal–oxygen fusion (MOXY) concept overcomes these limitations. When reviewing the literature on the many documented forms of LENRs, one particular strand of evidence stands out. In all forms of LENRs, if oxygen is not a constituent within the experimental apparatus, no fusion signature occurs. In other words, when oxygen is removed from these experiments, evidence of fusion ceases. Of all the experiments noted in the literature review, that of Ohsawa-Kushi (Nelson, 1998) seems the most promising to explain the LENR phenomenon.

After undertaking an extensive review of the literature, which is summarized in the following sections, the goal of this study was to confirm the findings of the Ohsawa-Kushi experiment and to demonstrate that the reproducible LENRs are the result of the MOXY fusion process. First, a brief review of other documented LENR processes that have produced fusion signatures is necessary for understanding MOXY.

A Brief Review of LENRs

Electrolytic LENRs with Platinum-Group Metals

A classic case of an electrolytic LENR is the Fleischmann-Pons "cold fusion" experiments (Fleischmann and Pons, 1989). Their experiments are typical of LENR electrolytic reactors, and they used platinum-group metals as anodes and cathodes. Fleischmann and Pons announced the results of their experiments publicly in 1989 and reopened the debate on LENRs in the scientific community. In their experiments, they claimed to have produced significantly more heat than the applied electrical input energy—and by an unknown process: "reaction (v) takes place to the extent of $1–2 \times 10^4$ atoms s^{-1} which is consistent with the measurements of the neutron flux. . . . [T]he data on enthalpy generation would require rates for reactions (v) and (vi) in the range of $10^{11}–10^{14}$ atoms s^{-1}" (Fleischmann and Pons, 1989, p. 305); additionally, "the bulk of the energy release is due to an hitherto unknown nuclear process or processes" (Fleischmann and Pons, 1989, p. 306). They theorized the fusion was taking place within the lattice of platinum-group metals when saturated with deuterium by an unknown process.

Some researchers claim to have reproduced Fleischmann and Pons' results of significant excess heat in their experiments, whereas others claim negative results (Krivit, 2005). Evidence of unknown nuclear synthesis processes has placed the Fleischmann-Pons–type of cold fusion into a state of speculation—and uncertainty. MOXY is likely the aforementioned "hitherto unknown nuclear process or processes" observed in this form of LENR electrolytic reactor.

Charge Cluster LENRs

Another type of LENR is produced within electrical discharge reactors through low-pressure gases or a vacuum. The charge cluster fusion described by the late Ken Shoulders is a classic example of this variety of LENR (Shoulders and Shoulders, 1996). A charge cluster is a vortex ring (Bulgac et al., 2014) of electrons—essentially, a spiraling loop of electrons and ions in a toroid-shaped flow. This vortex ring is also called a *soliton*. A soliton can be visualized as an electron/ion smoke ring. The electrodynamic

forces generated in the flow of spiraling electrons overcome the repulsive forces between electrons while spiraling in the outer part of the vortex ring. A soliton also can absorb atomic nuclei that spiral in the opposite direction of the electrons within the core of the vortex ring. A soliton might be classified as an exotic form of degenerate matter.

A typical charge cluster is ≈1 μm and is estimated to contain 10^{11} electrons, as well as between 10^5 and 10^6 ions (atomic nuclei). This ratio results in approximately 10^6 to 10^5 electrons for every ionized nucleon (Fox and Baily, 1997). An alternative way of conceptualizing this cluster is as a mass of electrons nearly equal to or exceeding the mass of baryons contained in the nuclei of 100 to 500 atomic masses, which well exceeds the mass of most nuclei involved. Therefore, it appears that the mass of electrons is significantly greater than the mass of baryons in soliton plasmas. The kinetic energy and magnetic fields of the electrons dominate the flow in the soliton, and ions are pulled within the flow, spiraling in an opposite direction from the electrons within the core of the electron smoke ring. This electron/ion flow can be characterized as an electrodynamic fluid. It has been suggested that solitons may come in quantized sizes (Fox, 1999), although more evidence is needed.

To effect this type of LENR, a charge cluster, or soliton, is produced from the tip of a pointed cathode, generated by a short, high-voltage pulse in a vacuum or low-pressure gas chamber. The soliton travels rapidly across the chamber toward the anode to impact targeted material. Microscopic examination of a soliton impact site reveals that a small crater is usually detected, a few micrometers across. A larger region of melted metal ejecta is concentric to the impact crater. In conductive metals, the craters are only a few micrometers deep. In dialectics and metal oxides, the craters can penetrate several millimeters into the substrate and infiltrate thin metal foils (Figures 1 and 2) (Shoulders and Shoulders, 1999).

(A)

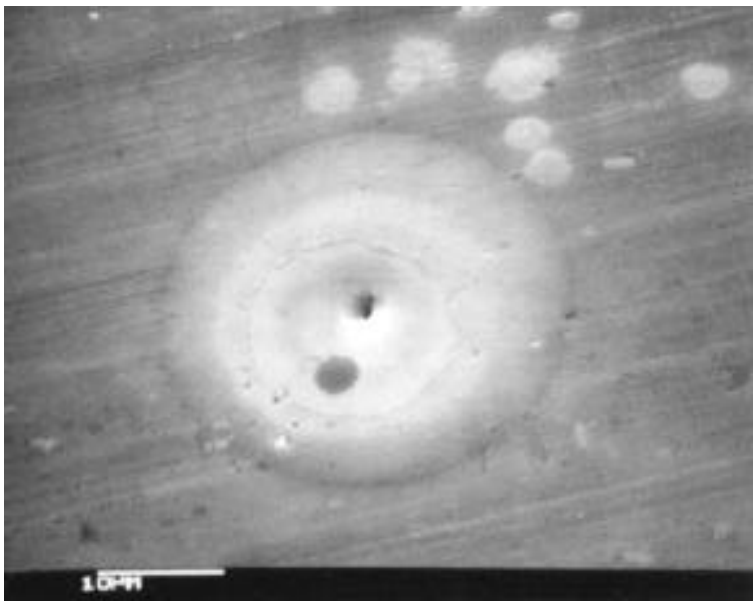

(B)

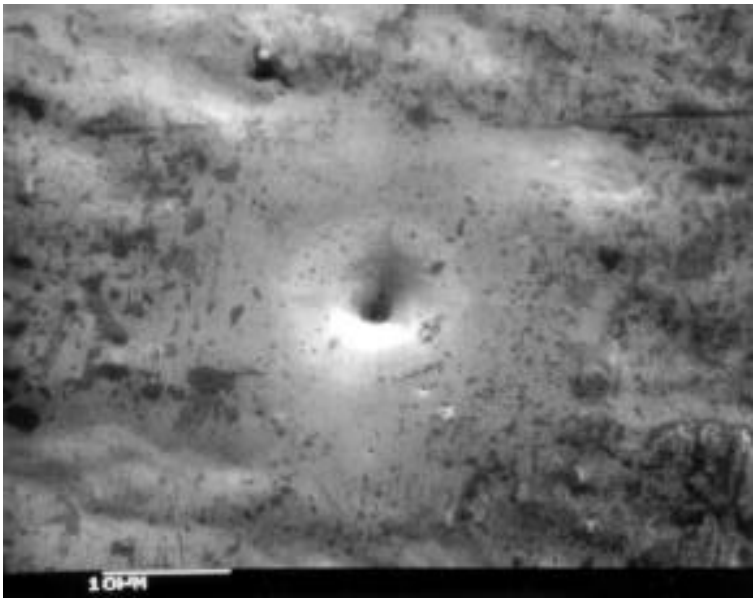

Figure 1. Highly organized, micron-size cluster of electrons strike a 6-μm-thick aluminum foil. (A) Entry side. (B) Exit side.
Source: Shoulders and Shoulders (1999)

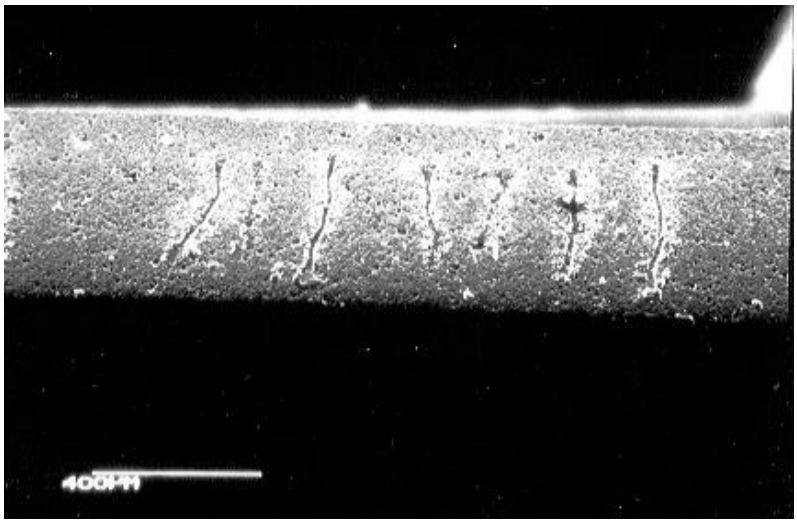

Figure 2. Cross section of boreholes of highly organized, micron-size clusters of electrons through a 0.5-mm-thick aluminum oxide plate.
Source: Shoulders and Shoulders (1999)

When a soliton impacts a highly purified metal and the impact site is examined under X-ray spectroscopy, no new elements are detected. However, when a soliton impacts a metal oxide surface on a metal, such as aluminum oxide, and the site is then examined under X-ray spectroscopy, new elements are detected (Shoulders and Shoulders, 1996, 1999). It is within the impact crater and ejecta melt that these new elements are detected (Shoulders and Shoulders, 1999). Evidence suggests that this form of LENR is the result of a MOXY process.

Another subset of the soliton phenomenon can be characterized as a charge vortex: the classic electric spark or tornado-like flow of electrons traveling between the cathode and anode. This charge vortex can also pull in ions when impacting the anode. The physical effects of a charge vortex impacting a metal is similar to a soliton, leaving pits and etching as it impacts and travels over the surface of the anode. Similar pitting is observed from lightning strikes on the metallic skin of airplanes (Fox, 1999).

Observations of atmospheric vortexes such as dust devils, water spouts, and tornadoes find the vast majority of the debris swept up by the vortex is located close to the outer wall, where flow is at a maximum. The outer wall is likely the location of ions in a charge vortex as it impacts an anode. If a charge vortex impacts a pure metal, and the

impact site is examined under X-ray spectroscopy, no new elements are detected. However, when a charge vortex impacts a metal oxide anode surface, new elements are detected by X-ray spectroscopy (Shoulders and Shoulders, 1999).

Direct-Current Field-Effect LENRs

A hybrid of the LENR phenomena discussed thus far occurs in electrolytic reactors and can be characterized as a soliton (or charge vortex) generated through dielectric breakdown, called a *field-effect emission*. This type of emission requires the presence of a valve metal as the anode plus a metal salt electrolyte (Fox, 1997). A metal oxide accumulates on the anode in the electrolytic cell environment and causes a significant increase in resistance at the electrode. It is thought that charge clusters form at the surface of the oxide layer, covering the anode by field emission, and then accelerate through the oxide layer during dielectric breakdown to impact the metal anode beneath it. Once again, when the impact site is examined under X-ray spectroscopy, new elements are detected.

Alternating-Current Field-Effect LENRs

Alternating-current (AC) field-effect LENRs also occur when a metal anode is coated by a metal oxide and is then switched to the cathode or, similarly, when the electrolytic cell operates with AC. Electrical resistance is greatly increased by the metal oxide covering the cathode, causing the cathode to glow and emit small sparks (Fox, 1997). It is thought that a soliton or a charge vortex forms at the metal oxide–metal boundary and erupts electrically through the oxide layer. This is observed as sparks emitting from the oxide layer. When the eruption/blast sites are examined under X-ray spectroscopy, new elements foreign to the experimental fixture are detected (Fox, 1997).

Alkali Metal Hydroxide LENRs

Another form of this hybrid LENR phenomenon occurs in electrolytic reactors using an alkali metal hydroxide such as potassium hydroxide (KOH) instead of a metal salt (Cirillo and Iorio, 2004). In extremely concentrated basic solutions, the positively charged alkali metal (K^+) migrates and accumulates around the cathode, as do hydrogen

ions and hydronium. These ions build up a shell of alkali metal around the cathode. Hydrogen/deuterium atoms are so small that they penetrate this metallic barrier, and electrolysis continues in the small gap between the cathode and alkali metal (Cirillo and Iorio, 2004).

After this alkali metal encasement occurs, the voltage is greatly increased, resulting in a gaseous, hydrogen-rich layer around the cathode. The greatly increased voltage, in conjunction with the increased electrical resistance, induce a plasma envelope around most of the cathode. Explosive electrical discharge events cause noticeable ablation of the cathode. When these ablated sites are examined with X-ray spectroscopy, new elements are detected (Cirillo and Iorio, 2004).

Alpha Particle Production with LENRs

Others have provided evidence, inadvertently, that the Fleischmann-Pons–type of cold fusion is possibly a result of MOXY. The experiments conducted by Oriana and Fisher (2003) are the best examples. They captured charged particles with passive alpha particle detectors suspended in the gases above a Fleischmann-Pons–type electrolytic cell. The electrolytic cell consisted of a palladium or nickel cathode surrounded by a spiral platinum anode. The electrolyte was lithium sulfate in deuterium oxide, and the electric current was between 0.1 A/cm^2 and 0.4 A/cm^2. The electrodes were submerged under several centimeters of the electrolyte, and a nickel plate was placed above the electrode to prevent direct alpha particle emission into the gas space above the electrolyte (Oriana and Fisher, 2003).

Alpha particles produced during the experiment were detected by four small CR-39 (i.e., Columbia Resin #39) plastic chips hanging from pairs of hooks attached to a rod suspended vertically several centimeters in the air above the electrolyte. (Similar plastic chips are used in residential applications to detect radon.) For Oriana and Fisher's experiment, the CR-39 chips were first treated with hot KOH solution to highlight any preexisting tracks created by alpha particles. These preprocessed chips were photographed carefully (Figure 3) and established the experiment's controls. The experiment proceeded over 3 days, with the four chips suspended in the atmosphere above the electrolyte. When the experiment was completed, the chips were again treated

with hot KOH and photographed (Figure 4). The beginning and ending photographs were compared to determine the number of alpha particles generated by vapors evaporating from the electrolyte.

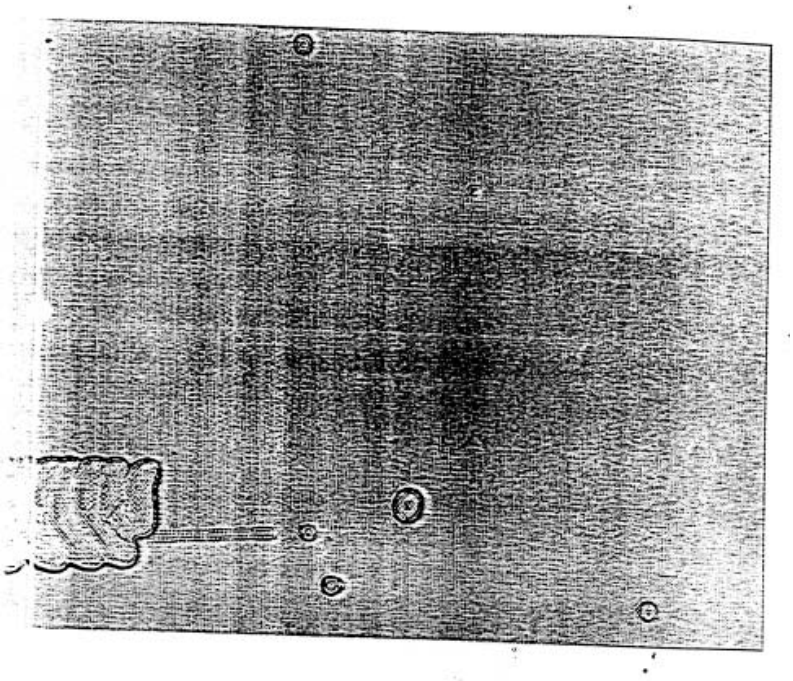

Figure 3. CR-39 plastic detector showing radon-produced nuclear tracks in the chip before exposure to electrolysis. The digital image was processed using a "Find Edges" computer application, with an original magnification of 100x. The feature in the lower left corner of the figure is a portion of a scratch.
Source: Oriana and Fisher (2003, Figure 2A)

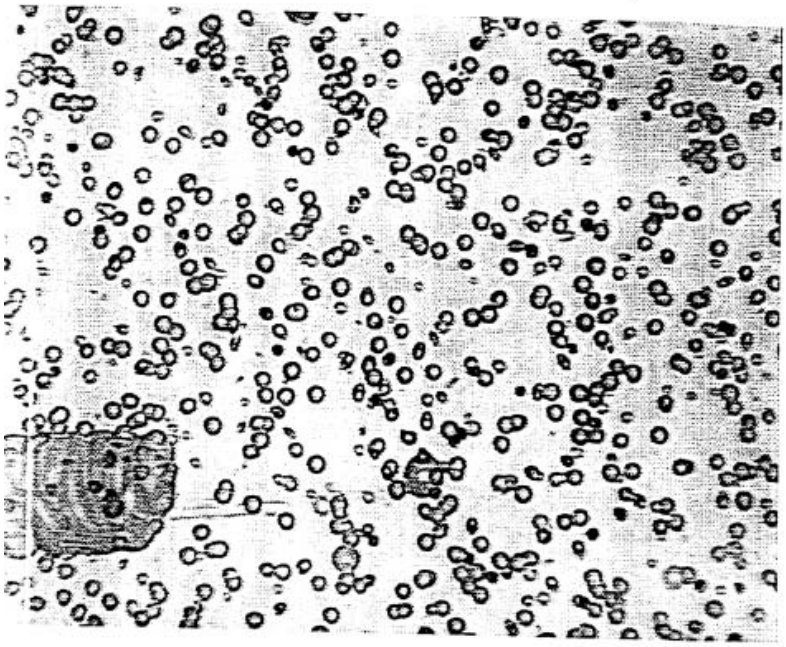

Figure 4. The same area after exposure of the CR-39 chip to electrolysis.
Source: Oriana and Fisher (2003, Figure 2B)

The results of the experiment by Oriana and Fisher showed 110 pits per image, compared to three pits per image in the control photos. The total density of pits in the experimental CR-39 chips was 176,000 pits/cm^2 compared with the 4,800 pits/cm^2 seen in the controls. Because the probability value that the results were produced by chance was $P = 3 \times 10^{-10}$, Oriana and Fisher (2003) concluded that "electrolysis can generate highly energetic charged particles by some kind of nuclear reaction that takes place in the gas phase." Other relevant observations were that the chips closer to the electrolyte appeared to receive slightly more charge particle radiation than chips mounted higher, and the source of emission appeared to be moving upward.

A question exists with regard to the nature of these numerous charged particles. Their emission signature resembles quite closely those of alpha particles. It is highly likely the charged particles recorded were indeed alpha particles, which the CR-39 chips were designed specifically to detect.

The source of the charged particles also appears to be in the air above the electrolyte. The observed alpha particles are unlikely to be coming directly from the

electrodes, because the nickel plate and several centimeters of electrolyte would absorb completely any alpha particles emitted from the electrodes. It is also unlikely the alpha particles are coming from the electrolyte in gaps between the nickel plate, because even a few millimeters of air will absorb most alpha particles. It is much more likely that alpha particles were generated by the radioactive decay of gases diffusing out of the electrolyte into the air above the electrolyte.

The MOXY fusion process postulates radioactive noble gases could be generated at the electrodes of this type of electrolytic cell. In the formulas that follow, the double dagger indicates a fusion event. The two most likely alpha-emitting noble gases are shown here from the most common isotopes of platinum (Pt) and palladium (Pd):

$$^{106}\mathrm{Pd} \ddagger {}^{16}\mathrm{O} \rightarrow {}^{122}\mathrm{Xe}$$

$$^{195}\mathrm{Pt} \ddagger {}^{16}\mathrm{O} \rightarrow {}^{211}\mathrm{Rn}$$

The first gas is xenon-122 (^{122}Xe), with a half-life of 20.1 hours. The second gas is radon-211 (^{211}Rn), which has a half-life of 14.6 hours. Both are noble gases with high vapor pressures and few chemical affinities. As noble gases, they have the potential to degas rapidly from a liquid electrolyte.

The electrolytic cell also generates oxygen and deuterium gases during electrolysis, producing a gas outflow from the electrolyte. This outflow of gas would assist in the diffusion of any generated radioactive noble gases into the upper section of the reactor, which in the experiment of Oriana and Fisher (2003) contained the CR-39 chips. This gas flow and dispersion could explain the appearance of alpha particles moving upward and, perhaps, could provide a reason for less pitting exhibited by the higher-positioned CR-39 chips.

When ionized alpha particles cool, they become helium-4 (^{4}He). This might also account for the ^{4}He detected in the Fleischmann-Pons–type of experiments—an observed and more likely source of ^{4}He than a hypothesized cold fusion or deuterium/deuterium fusion.

Beginning in the 1980s and in experiments still being done today, nearly all of the radioactive gases generated exit the electrolytic cell long before decaying and mixing with the air in the laboratory. Any scientists conducting these experiments have inhaled this highly contaminated air. Many scientists who conducted extensive Fleischmann-Pons–types of cold fusion experiments have died prematurely, including Dr. Fleischmann.

Materials and Methods

After an examination of the extensive literature on LENR/fusion reactions, the Ohsawa-Kushi experiments (Nelson, 1998), which are summarized here, seem the most promising pathway to follow for successful fusion. These experiments were well designed, described a plausible fusion process, and clearly showed a path to positive results. Another advantage is that the experiments were based on the use of oxygen as a fusing element in conjunction with a metal. For these reasons, an Ohsawa-Kushi fusion experiment was chosen for reproduction.

The Ohsawa-Kushi experiment targeted for reproduction was the fusion of sodium and oxygen into potassium. Ohsawa and Kushi had concluded that fusion occurred when the red-violet spectral line of ionized potassium appeared and eventually came to dominate the yellow, sodium-produced light emitted from their reactor (Nelson, 1998).

Some modifications to the Ohsawa-Kushi experiments were necessary, although each modification strictly followed the principles of Ohsawa and Kushi. The first modification was to replace sodium with deuterium. Because these elements are in the same atomic family, they should behave in a similar manner in the experiment, according to the Ohsawa-Kushi principles. Metallic sodium and sodium oxide are hazardous and difficult to work with, especially in the presence of moisture. Working with deuterium oxide is far easier and safer. Heavy water is a plentiful and available industrial material. A deuterium/oxygen fusion would also produce a much greater release of binding energy than a sodium/oxygen fusion. The second modification was to maintain near-atmospheric pressure in the reactor vessel, rather than the pressure realized in a low-pressure reactor chamber.

With the change in elements, the red-violet spectral line of potassium would no longer be present as an indicator of fusion. Therefore, the third modification to the Ohsawa-Kushi experiment was to substitute X-ray digital plates to record emissions from the expected fusion events. Another reason to use X-ray digital plates is the electric spark discharge that occurs during the experiment. The spark discharges hundreds to thousands of times per second and produces powerful radio frequency (RF) radiation. These RF

emissions will overwhelm any Geiger counter or similar device designed to detect ionizing radiation. X-ray digital plates are unaffected by strong RF emissions. Both the reactor vessel and the electronics producing the electric spark need to be contained within a robust Faraday cage to prevent this RF disruption. In third-party confirmation testing of MOXY fusion, several frequencies in the X-ray band and low gamma-ray bands were detected with a multichannel sodium iodine detector.

The modification of this MOXY reaction through the substitution of sodium-23 (^{23}Na) with deuterium-2 (^{2}D) is shown in the following equations (again, the double dagger indicates a fusion event):

$$^{23}\text{Na} \ddagger {}^{16}\text{O} \rightarrow {}^{39}\text{K} + \gamma$$

to

$$^{2}\text{D} \ddagger {}^{16}\text{O} \rightarrow {}^{18}\text{F} \ddagger \text{EC} \rightarrow {}^{18}\text{O} + \nu + \gamma$$

where ^{16}O is oxygen-16, ^{39}K is potassium-39, ^{18}F is fluorine-18, EC refers to electron capture, ^{18}O is oxygen-18, γ indicates gamma rays, and ν reflects neutrinos.

Per the previous equations, hypothetically, after each of the two lighter elements fuse into a heavier element, the resulting excited nucleus drops into a ground state through the emission of an X-ray/weak gamma ray. In the case of the principal reaction path, the resulting ^{18}F is unstable and likely decays rapidly through EC (or possibly positron emission) into ^{18}O and emits a neutrino to balance spin. An X-ray/weak gamma ray is also emitted, along with the kinetic energy added to the nucleus, during the drop to stable ^{18}O. This deuterium–oxygen fusion pathway emits much less energy than the binding energy release of the deuterium ‡ deuterium = ^{4}He pathway of 23.8 MeV or the energy of the ^{3}He ‡ deuterium = ^{4}He + *n* at 18.4 MeV pathway, where *n* refers to a neutrino.

Results

MOXY reactor experimentation was conducted under strict Ohsawa-Kushi protocols. The cathode was fabricated from copper and the anode from iron. The glass reactor chamber was filled with an argon atmosphere, with deuterium oxide evaporated into it from an internal reservoir to saturation vapor pressure (≈7%). When the electric spark was activated, copious amounts of X-rays were detected, and they were recorded using digital X-ray film common to dentistry. The electric spark was only capable of sparking across a 4 mm gap (or shorter) in ordinary atmosphere, which indicates energy at ≈4 kV. A minimum of 10 kV is needed to produce the weakest of X-rays. This potential 4 kV voltage is reduced further in more conductive argon gas ($V = IR$, where V is argon gas, I is deuterium water, and R is vapor in the reactor air), making it highly unlikely for the electric spark to be the source of the X-rays. This phenomenon was also supported by the argon gas-only experiment, producing no X-rays.

If any of the required experiment components were absent, X-rays should not be produced. The first control was the electric spark or charge vortex discharging through normal atmosphere, when no X-rays should be recorded. The atmosphere of the laboratory contained between 3% and 4% humidity of ordinary water. Another control was the charge vortex operating in an argon-only atmosphere, where again, no X-rays should be recorded. A further control was the electric spark operating with heavy water in ambient atmosphere without argon; again, no X-rays should be recorded. And they were not.

These controls were conducted repeatedly. Only when all the Ohsawa-Kushi parameters were in place were X-rays recorded. In addition, when the anode became submerged in heavy water during the experiments, although the electric spark continued to discharge to the surface of the heavy water, no X-rays were recorded. This result suggests that fusion was occurring on the surface of the anode. The iron anode could be characterized as an electrofusion catalyst when in an argon–deuterium oxide atmosphere and under electric spark discharge.

In the MOXY reactor, the X-ray emissions appeared to be continuous and copious, completely blackening the large digital X-ray plate in less than an hour

(Figure 5). These X-ray results tend to confirm an Ohsawa-Kushi fusion transmutation hypothesis and suggest that a previously unknown nuclear fusion process based on oxygen and a metal is occurring. In this case, because deuterium is in the alkali metal family, it is considered a metal. Hydrogen does act as a metal under high pressure or in degenerate matter. Hence, this is considered a MOXY process. Additional confirmation of these MOXY experiments awaits further metrics. Spectroscopic measurements of ^{18}O concentrations within the reactor, in comparison to the heavy water source, need to be conducted.

(A)

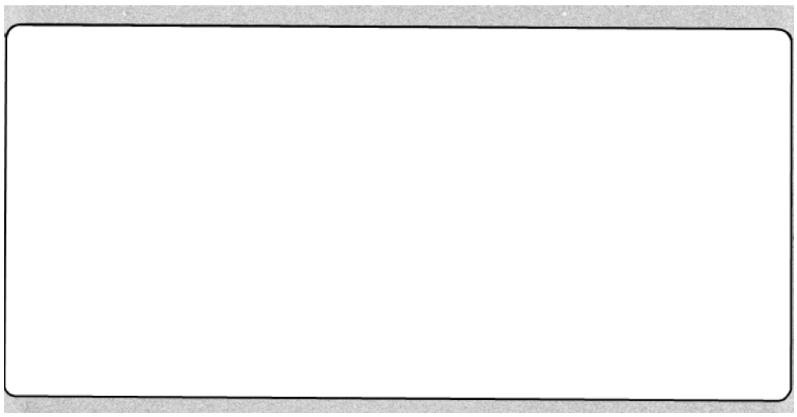

(B)

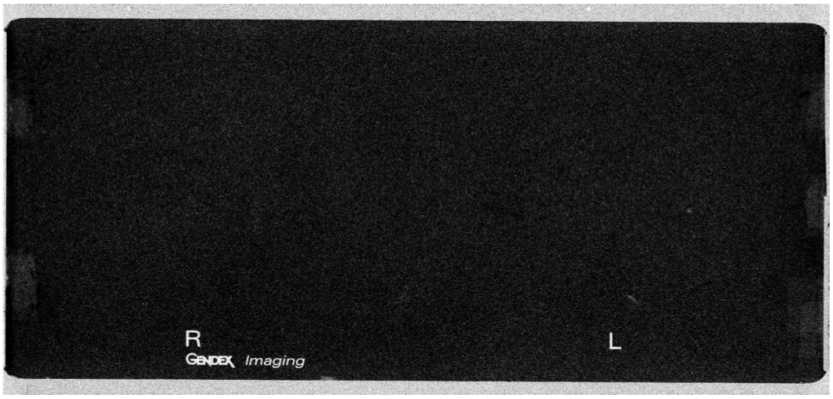

Figure 5. (A) Typical example of unexposed Gendex digital panoramic X-ray imaging from controls. **(B)** One-hour exposure of the Gendex digital X-ray plate to the MOXY reactor.
Both images acquired February 7, 2014

Absorption parameters of the digital X-ray film limited the detected X-rays to less than 200 kV in energy (Szpak et al., 2005). The two types of X-ray digital panels used were a Gendex 2010-01, a barium fluorobromine (BaFBr)–based detector ≈10 cm^2 in area, and a Gendex panoramic gadolinium oxysulfide (Gd_2O_2S)–based detector ≈560 cm^2 in area. Because the Gendex technical data are unavailable as of this writing, the X-ray absorption profile of similar Kodak panels is shown in Figure 6, in which GP corresponds to the panel Gd_2O_2S and HR corresponds to the panel BaFBr.

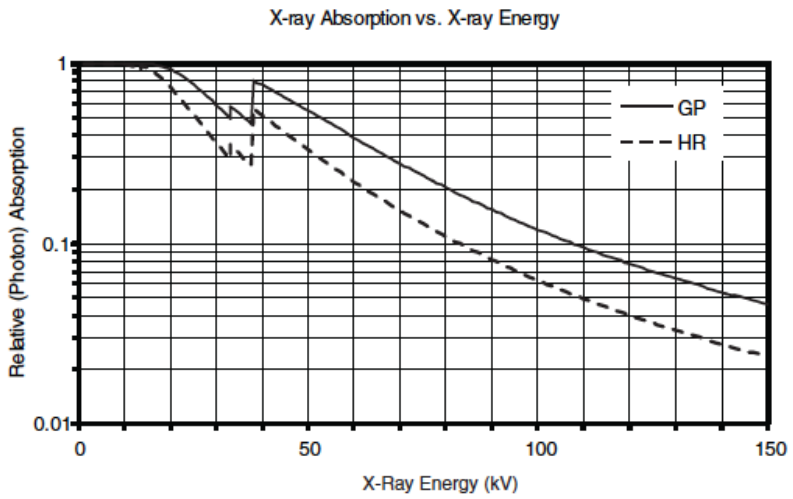

Figure 6. Kodak photodetector panel absorption profiles.

Discussion

The emission of X-rays in Fleischmann-Pons electrolytic-type cells and other cell types has been detected using different detection methods by several researchers. The detection of X-rays is episodic and often weak, stretching over a timeline of days. X-ray bursts accompanied by excess heat have been observed (Iwamura et al., 1996). Some of these episodic emissions of X-rays have been found to be directional (Szpak et al., 1991).

An interesting phenomenon led to X-ray digital film being chosen to look for the signature of fusion events, rather than a Geiger counter. It has been demonstrated experimentally (Bosch et al., 1996) that the half-life of fully ionized rhenium-187 (^{187}Re) is decreased by 9 orders of magnitude over neutral ^{187}Re to 33 years, from 42 billion years. The barrier for an energetic electron beta emission from the nucleus reduced by 1.3 billion–fold. This is a significant increase in beta decay rates for converting ^{187}Re into osmium-187 (^{187}Os). Interestingly, the resulting beta emission is so weak the electron is captured in the K shell, the lowest electron shell (Bosch et al., 1996). Energy emissions from the resulting, excited ^{187}Os nucleus were inferred to be significantly less than from nonionized ^{187}Re beta decay, although they were not measured.

Beta decay is characteristic of daughter elements generated from atomic fission containing an excess of neutrons required for atomic nucleus stability. An excess neutron is converted into a proton through beta decay, *producing a more stable daughter product one element higher on the atomic chart*. Beta emissions are produced at a wide variety (bell curve) of energies, and the neutrino is held to carry off the balance of the energy. Beta decay could be characterized as an energetic electron emission from the nucleus. In cases of extreme neutron imbalance, a neutron can be emitted from the nucleus, moving toward nuclear stability.

If a dearth of electrons could assist in the emission of beta particles, perhaps an excess of electrons, such as that found in a soliton, might increase the probability of fusion, EC, alpha decay, and proton emission from a nucleus—and by orders of magnitude. This excess of electrons would also likely reduce the probability of positron emission from the nucleus. Any electromagnetic radiation produced by the resulting

excited nucleus would likely be significantly reduced as well, potentially moving any fusion signature from the gamma-ray band into the X-ray band.

The stability of atomic nuclei is sensitive to the ratio of neutrons to protons. Fusion tends to generate an excess of protons or lack of neutrons for atomic stability, especially moving toward the higher elements. The proton-to-neutron ratio for elements starts out at about 1:1, but approaches a ratio of 1:1.5 as one advances toward heavier elements and elements with higher electron shell levels. Unstable fusion products move toward stability by positron emission, EC, alpha decay, and proton emission. This is quite the opposite of unstable fission products, which move toward stability by neutron emission and beta decay, as seen in Figure 7.

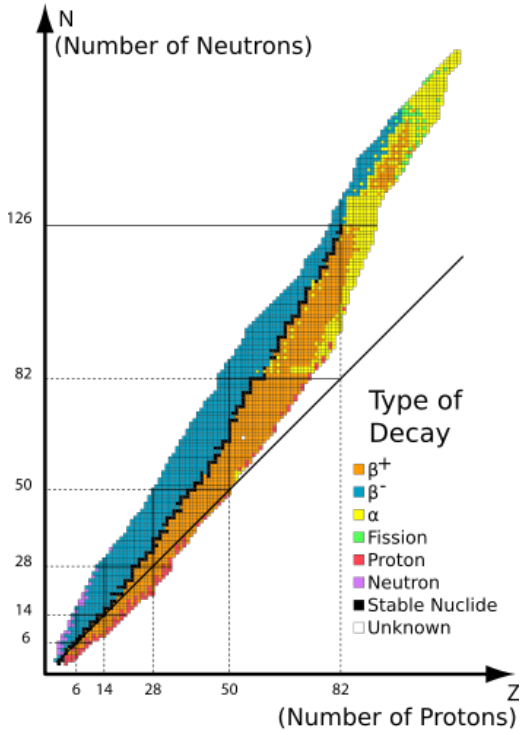

Figure 7. Types of nuclear decay atomic stability chart.
Source: n.a., 2020. Stable nuclide. https://en.wikipedia.org/wiki/Stable_nuclide (accessed July 8, 2020)

Calculating the Coulomb barrier that determines penetration of a nucleus relies on two conditions. First, particles are seen as point charges, and these charges must be stationary with respect to one another. The second condition of stationary relationships does not exist in a rapidly spiraling soliton of many LENRs. The velocity of ions swept up in a soliton vortex can be high, but nowhere near relativistic velocities.

Fusion is a tunneling process, and the closeness of the baryons/nuclei increases its probability exponentially. The charge environment of these high electron masses to baryonic masses in solitons resembles, in some ways, the state of degenerate matter found in stellar cores, where fusion is known to occur. Degenerate matter exists when great pressure has pushed electrons much closer to the nucleus, increasing the negative charge density. There is some evidence of increased alpha decay resulting from greater electron density. In samarium-147 (^{147}Sm), the presence of a full electron shell increases the probability of alpha decay 2.6-fold when compared to a fully ionized nucleus (Urutskoev and Filippov, 2010). This increased alpha decay with greater electron density might also extend into EC and proton emission.

It is possible that the high electron charge density and the dynamic vortex flow of a soliton associated with aligned, strong magnetic fields may lower the Coulomb barrier, allowing fusion to occur, as well as protons and alpha particles to escape, or permitting electrons to be captured by an excited nucleus. It is also possible that relatively low-energy plasma collisions might induce fusion. In a soliton, the mass of electrons is significantly heavier than the baryonic mass of the ions, and it exceeds the charge–density relationship of degenerate matter.

The charge–mass relationship is far more balanced in the electrodynamic fluid of the soliton compared to the usual electron–proton mass ratio of 1:1,836 in common degenerate matter. When the soliton impacts the anode, the soliton is greatly compressed by the electron shells of the anode atoms. This tends to squeeze any nuclei within the soliton much closer together, increasing the possibility of tunneling exponentially and increasing the possibility for fusion to occur.

A Coulomb barrier reduced by orders of magnitude should also result in a much lower emission frequency from excited fusion-synthesized nuclei. In stars, fusion occurs at millions of degrees centigrade, and daughter nuclei are very excited. Any MOXY

emissions would likely be in the X-ray energies, rather than an expected megaelectron, volt-level gamma emission. The rest of the binding energy is expressed in the kinetic energy of the resulting nucleon and, in some cases, by a neutrino as well. When released, this binding energy might be detected as an increase in heat within the reactor. During MOXY testing, the reactor was surrounded by ice, because less than a minute of operation would heat the gases within the reactor to become so thin the electron spark could no longer conduct. This never occurred with the controls when the necessary constituents for an Ohsawa-Kushi protocol reaction were not present.

The MOXY hypothesis underlying the modified Ohsawa-Kushi experiment appears to be partially confirmed through the production of copious X-rays when the soliton electrical discharge was activated. A nearly indisputable confirmation depends on spectroscopic measurement of a relative increase in the ^{18}O concentration within the reactor, in comparison to the heavy-water source or through the detection of new elements within the iron anode.

Several varieties of MOXY fusion may be occurring at the iron anode as a result of the several different isotopes of iron. Spectroscopic analysis of the iron anode is necessary to confirm any of these proposed MOXY fusion pathways and is not currently available from the literature. However, many new elements have been observed with X-ray spectroscopy using similar electrode metals with LENRs (Dash and Warner, 2000).

Based on an examination of the LENR literature for the first three electron shell levels (K, L, and M), the fusion pathways appear, in general, to conform to the standard model. However, the MOXY fusion pathways also appear to grow increasingly complex and exotic by the fourth electron shell. Progressing toward the seventh electron shell level, the complexity and variety of MOXY fusion synthesis and decay pathways appear to increase significantly. This may be a result of the MOXY fusion products having low levels of excitation and binding energy for stability.

The MOXY fusion process also appears to become increasingly easier to induce with greater atomic mass. The exotic nature of MOXY, when compared to the corpus of the standard model, coupled with rapidly increasing complexity, is another source that currently frustrates researchers from gaining an understanding of LENRs.

Inside a soliton, the plasma comes to resemble more the degenerate matter found in stellar cores, especially when impacting the anode. This permits low-probability tunneling fusion events to become more common. Hitherto unknown nuclear synthesis and decay pathways also become manifest in resulting daughter products. The possible appearance of double alpha decay, triple alpha decay, and beryllium-9 (^{9}Be) decay are a few example products of these events (Dash and Warner, 2000). In all the following cases of new elements being detected through some type of LENR process, oxygen is always present.

A series of LENR experiments conducted at Portland State University was designed well and documented in detail (Cirillo and Iorio, 2004; Kopecek and Dash, 1996). Their experiments used titanium or palladium electrodes in a sulfuric acid/heavy-water electrolyte. Titanium is at the same fourth atomic shell level as iron and is a valve metal. Both types of experiments used a platinum anode. After use, the titanium and palladium electrodes contained new elements in localized areas that were detected by energy-dispersive X-ray spectroscopy. These authors labeled the new elements “unexpected elements” (Kopecek and Dash, 1996).

The experiments of Kopecek and Dash (1996) help characterize the possible MOXY fusion pathways likely occurring on the iron anode. The titanium cathode can be characterized as an electrofusion catalyst similar to the alkali metal hydroxide LENRs described earlier.

The detected unexpected elements heavier than titanium were vanadium, chromium, iron, nickel, and zinc (Kopecek and Dash, 1996). No elements heavier than zinc were detected, and all support an oxygen-based fusion process, as fused titanium and oxygen produce zinc as the heaviest possible product. These unexpected metals were found in the craters and the ejecta melt only, and in various concentrations relative to each other, depending on the localized region examined by energy dispersive X-ray spectroscopy. Table 1 shows some of the unexpected element ratios detected by Dash and his graduate student Kopecek (Dash and Warner, 2000; Kopecek and Dash, 1996).

Table 1. Results of Electrolysis of Deuterium Oxide with Titanium Cathodes

Region	Titanium (%)	Vanadium (%)	Chromium (%)	Iron (%)	Nickel (%)	Zinc (%)
1	93		3	5	Trace	
2	100					
3		4*				
4	100					
5	99		1	Trace		
6	89		10	1		
7	79	9	2			

Data from Dash and Warner (2000) and Kopecek and Dash (1996)
*No ancillary data provided

Titanium has several stable isotopes: titanium-50 (^{50}Ti) at 5%, ^{49}Ti at 5%, ^{48}Ti at 73%, ^{47}Ti at 7%, and ^{46}Ti at 8%. This implies a wide variety of possible isotopes generated by a MOXY process. Unfortunately, Kopecek and Dash (1996) did not measure the isotopic signature of the unexpected elements. With the MOXY fusion process, zinc is expected to be the heaviest new element produced, and it was the heaviest new element detected. A rather complex set of potential MOXY nuclear synthesis and decay pathways is possible.

The pathways follow these potential MOXY nuclear synthesis pathways (the asterisk indicates an unstable isotope):

$$^{50}\text{Ti} \ddagger {}^{16}\text{O} \rightarrow {}^{66}\text{Zn} + \gamma$$

$$^{49}\text{Ti} \ddagger {}^{16}\text{O} \rightarrow {}^{65}\text{Zn}^*$$

$$^{48}\text{Ti} \ddagger {}^{16}\text{O} \rightarrow {}^{64}\text{Zn} + \gamma$$

$$^{47}\text{Ti} \ddagger {}^{16}\text{O} \rightarrow {}^{63}\text{Zn}^*$$

$$^{46}\text{Ti} \ddagger {}^{16}\text{O} \rightarrow {}^{62}\text{Zn}^*$$

Of the zinc produced, zinc-66 (^{66}Zn) and ^{64}Zn are potentially stable, whereas ^{65}Zn, ^{63}Zn, and ^{62}Zn are unstable and, under the standard model, would positron/EC decay into copper. However, no copper was detected. According to Table 1, the synthesis of zinc was the least evident. In the degenerate environment of MOXY fusion, these nucleons would be excited, but still might have less energy than necessary for stability.

It is possible that alpha decay is the easiest pathway to increase nuclear stability with MOXY. There is some support for this alternative alpha decay pathway, as ^{147}Sm has a 2.6-times faster alpha decay rate over a fully ionized ^{147}Sm nucleus (Urutskoev and Filippov, 2010). It could follow the potential nuclear decay pathways of:

$$^{50}Ti \ddagger {}^{16}O \rightarrow {}^{66}Zn \rightarrow {}^{62}Ni + \alpha + \gamma$$

$$^{49}Ti \ddagger {}^{16}O \rightarrow {}^{65}Zn \rightarrow {}^{61}Ni + \alpha + \gamma$$

$$^{48}Ti \ddagger {}^{16}O \rightarrow {}^{64}Zn \rightarrow {}^{60}Ni + \alpha + \gamma$$

$$^{47}Ti \ddagger {}^{16}O \rightarrow {}^{63}Zn \rightarrow {}^{59}Ni^*$$

$$^{46}Ti \ddagger {}^{16}O \rightarrow {}^{62}Zn \rightarrow {}^{58}Ni^*$$

Nickel-63 (^{63}Ni), ^{62}Ni, ^{61}Ni, and ^{58}Ni are stable isotopes, but ^{59}Ni is unstable and positron/EC decays into cobalt. However, no cobalt was detected. As seen in Table 1, only a trace of nickel was detected. It is conceivable that unstable zinc might double alpha decay into iron with MOXY. Double alpha decay is highly improbable, but it has been observed, and it could follow the potential nuclear decay pathways of:

$$^{50}Ti \ddagger {}^{16}O \rightarrow {}^{66}Zn \rightarrow {}^{58}Fe + 2\alpha + \gamma$$

$$^{49}Ti \ddagger {}^{16}O \rightarrow {}^{65}Zn \rightarrow {}^{57}Fe + 2\alpha + \gamma$$

$$^{48}Ti \ddagger {}^{16}O \rightarrow {}^{64}Zn \rightarrow {}^{56}Fe + 2\alpha + \gamma$$

$$^{47}Ti \ddagger {}^{16}O \rightarrow {}^{63}Zn \rightarrow {}^{55}Fe^*$$

$$^{46}Ti \ddagger {}^{16}O \rightarrow {}^{62}Zn \rightarrow {}^{54}Fe + 2\alpha + \gamma$$

Iron-58 (^{58}Fe), ^{57}Fe, ^{56}Fe, and ^{54}Fe are stable isotopes, but ^{55}Fe is unstable and positron/EC decays into manganese. However, no manganese was detected. To explain the unexpected element of chromium, a nonstandard model nuclear decay pathway of triple alpha decay would need to be invoked. It could follow the potential MOXY nuclear decay pathways of:

$$^{50}Ti \ddagger {}^{16}O \rightarrow {}^{66}Zn \rightarrow {}^{54}Cr + 3\alpha + \gamma$$

$$^{49}Ti \ddagger {}^{16}O \rightarrow {}^{65}Zn \rightarrow {}^{53}Cr + 3\alpha + \gamma$$

$$^{48}Ti \ddagger {}^{16}O \rightarrow {}^{64}Zn \rightarrow {}^{52}Cr + 3\alpha + \gamma$$

$$^{47}Ti \ddagger {}^{16}O \rightarrow {}^{63}Zn \rightarrow {}^{52}Cr + 3\alpha + \gamma \rightarrow {}^{51}Cr \ddagger EC \rightarrow {}^{51}V + n + \gamma^*$$

$$^{46}Ti \ddagger {}^{16}O \rightarrow {}^{62}Zn \rightarrow {}^{50}Cr + 3\alpha \rightarrow + \gamma$$

Chromium-54 (^{54}Cr), ^{53}Cr, ^{52}Cr, and ^{50}Cr are stable isotopes, but ^{51}Cr is unstable and could EC decay into vanadium to achieve stability, and some vanadium (vanadium-51 [^{51}V]) was detected. Interestingly, from the spectroscopic results, chromium from triple alpha decay is one of the most common alpha decay pathways. This is a series of quite fanciful and hypothetical MOXY nuclear decay pathways, and which, if any, is accurate remains unknown. However, they have the potential to suggest explanations for the unexpected elements heavier than the titanium that Dash and colleagues detected (Dash and Warner, 2000).

In another set of experiments by Dash and colleagues, the ratios of the titanium isotopes relative to one another were measured before and after the experiments (Kozima et al., 2002). From the data, it appears that titanium isotopes with more neutrons had a greater propensity to fuse by the MOXY process, as shown in Table 2.

Table 2. Titanium Cathodic Isotope Ratios after Deuterium Oxide Fusion

Isotope	Ti Cathode Before	Ti Cathode After	In Electrolyte After
$^{50}Ti/^{45}Ti$	0.6960	0.6683	0.6593
$^{50}Ti/^{47}Ti$	0.8027	0.6978	0.7022
$^{50}Ti/^{48}Ti$	0.0785	0.0727	0.0685
$^{50}Ti/^{49}Ti$	1.0111	0.9358	0.9476

Source: Kozima et al. (2002)

These and similar LENR experiments were conducted using palladium electrodes and resulted in the generation of excess heat—and unexpected elements (Dash and Miguet, 1996; Kopecek and Dash, 1996; Mallove, 1995; Mizuno et al. 2000; Szpak et al. 2005). Palladium is similar to titanium in having several stable isotopes, but

it is at the fifth electron shell level. The palladium electrodes produced much less heat with respect to power input and, on closer examination, showed much less ablation. These palladium electrodes also had small deposits at the localized areas: fibers of unexpected elements and generalized deposits of platinum from the anode (Kopecek and Dash, 1996). The fibers may have come from graphite cloth used in the reactor. These fibers also contained palladium, sulfur, and oxygen (Kopecek and Dash, 1996).

The unexpected elements heavier than palladium that were detected were silver and cadmium (Dash and Miguet, 1996; Kopecek and Dash, 1996), which are equivalent in elemental relation to the chromium and vanadium detected on the titanium electrode.

As discussed earlier in regard to the Fleischmann-Pons–type experiment, there is the potential MOXY pathway of:

$$^{106}\mathrm{Pd} \ddagger {}^{16}\mathrm{O} \rightarrow {}^{122}\mathrm{Xe}$$

which is the elemental equivalent of zinc with titanium. Xenon would not be detected by X-ray spectroscopy of the electrodes. No elements heavier than a potential palladium oxygen fusion were detected.

Cooled alpha particles from the numerous alpha decay pathways soon became $^{4}\mathrm{He}$. This could explain the detection of $^{4}\mathrm{He}$ from these types of LENR reactors. MOXY is a far more likely alternative source of $^{4}\mathrm{He}$ production over the improbable pathway of deuterium/deuterium fusion with its undetected highly energetic gamma rays.

The final metal missing in the MOXY synthesis chain is antimony, the equivalent of nickel with titanium. Antimony is a chemically reactive element (as is zinc) and, in a sulfuric acid electrolyte, tends to dissolve rapidly.

From the experimental data, there appear to be some parallels between the MOXY fusion pathways of titanium and palladium, although they vary in the unexpected elements of heavier potential. This may be attributed to MOXY fusion and decay processes that become more complex in elements that feature increasingly higher electron shell levels.

Electrodes used in some LENRs appear to take quite a battering at the nucleonic level. Under the MOXY hypothesis, electrodes can act as electrofusion catalysts. Six weeks after conducting a Fleischmann-Pons–type experiment, the late

Dr. Kevin Wolf of Texas A&M discovered that his palladium electrodes were mildly radioactive. The isotopic ratio was also different from those obtained from bombardment by high-energy beams of deuterium or protons (Mallove, 1995; Passell, 1995). All the isotopes are within one element above, to two elements below, palladium. The isotopes are shown in Figure 8, along with hypothesized production pathways.

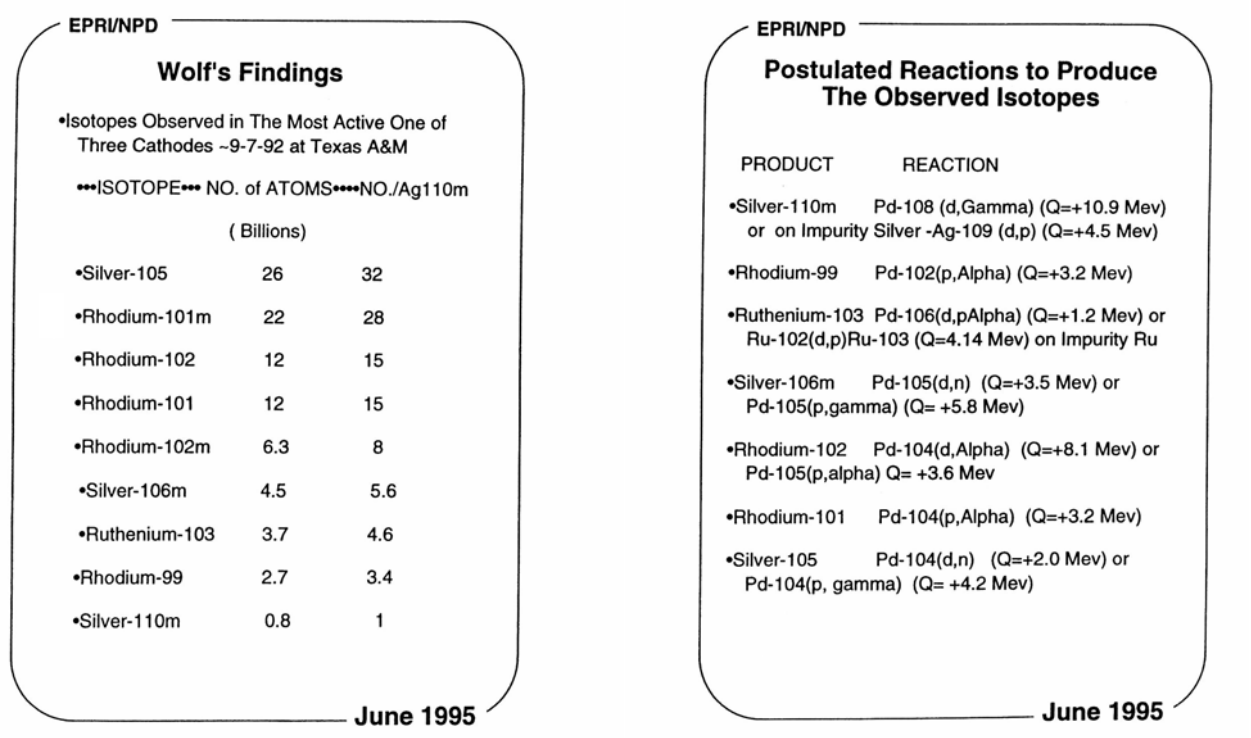

EPRI/NPD

Wolf's Findings

•Isotopes Observed in The Most Active One of Three Cathodes ~9-7-92 at Texas A&M

•••ISOTOPE•••	NO. of ATOMS (Billions)	••••NO./Ag110m
•Silver-105	26	32
•Rhodium-101m	22	28
•Rhodium-102	12	15
•Rhodium-101	12	15
•Rhodium-102m	6.3	8
•Silver-106m	4.5	5.6
•Ruthenium-103	3.7	4.6
•Rhodium-99	2.7	3.4
•Silver-110m	0.8	1

June 1995

EPRI/NPD

Postulated Reactions to Produce The Observed Isotopes

PRODUCT	REACTION
•Silver-110m	Pd-108 (d,Gamma) (Q=+10.9 Mev) or on Impurity Silver -Ag-109 (d,p) (Q=+4.5 Mev)
•Rhodium-99	Pd-102(p,Alpha) (Q=+3.2 Mev)
•Ruthenium-103	Pd-106(d,pAlpha) (Q=+1.2 Mev) or Ru-102(d,p)Ru-103 (Q=4.14 Mev) on Impurity Ru
•Silver-106m	Pd-105(d,n) (Q=+3.5 Mev) or Pd-105(p,gamma) (Q= +5.8 Mev)
•Rhodium-102	Pd-104(d,Alpha) (Q=+8.1 Mev) or Pd-105(p,alpha) Q= +3.6 Mev
•Rhodium-101	Pd-104(p,Alpha) (Q=+3.2 Mev)
•Silver-105	Pd-104(d,n) (Q=+2.0 Mev) or Pd-104(p, gamma) (Q= +4.2 Mev)

June 1995

Figure 8. Passell's quotation of radiation data reported by Wolf at Texas A&M. *Source*: Passell (1995)

Palladium has six stable isotopes from which these radioactive isotopes were synthesized. Nearly all these isotopes follow a positron/EC decay pathway, along with single beta decay. This implies they move toward stability while maintaining their atomic mass number. The produced isotope abundance does not follow a known standard model of a nuclear synthesis pathway, so a chart showing their relationship to stable nucleons is provided in Figure 9.

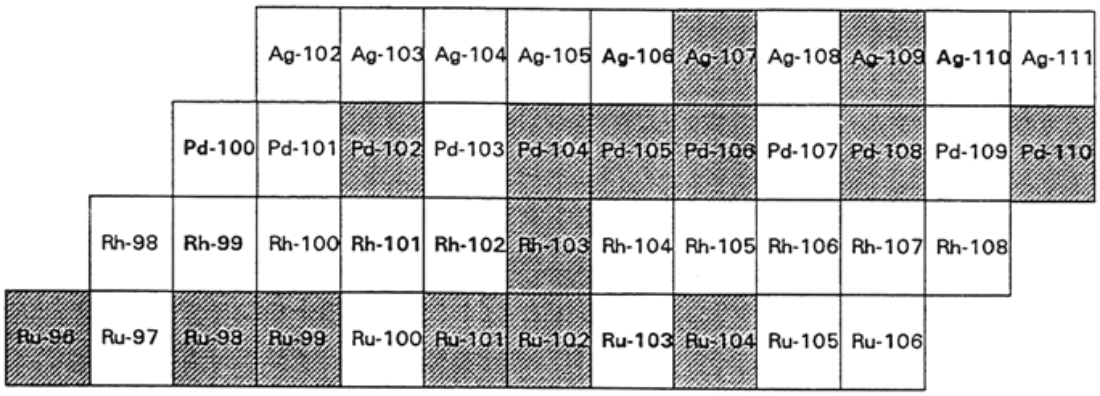

Figure 9. Cold fusion experiment transmuted heavy element distribution.
Source: Mallove (1995)

In Wolf's experiment, it appears that most of the isotopes were formed by the addition of a single baryon or, perhaps, a double baryon (deuterium) (Passell, 1995). This baryonic gain might be a result of palladium acting as an electrofusion catalyst. If a greater electron density increases alpha decay, it likely would also increase the probability of proton emission, as a first emission after fusion. In some cases, an electrofusion catalyst might absorb this proton. The isotopes of ruthenium may have been formed by alpha decay, produced from palladium made unstable as a result of the addition of baryon. Calcium was also found (Passell, 1995) in the unexpected elements detected in the localized area on the titanium electrodes, which could be a result of alpha decay from an unstable titanium isotope (Kozima et al., 2002; Dash and Warner, 2000).

Several potential exotic decay pathways appear to occur when using tungsten as a cathode/electrofusion catalyst in an alkali KOH electrolyte. Tungsten is at the sixth electron shell level. The potassium in the electrolyte encases the electrode. Temperatures between 10,000°C and 34,000°C are produced on the surface of the electrode when electrical energy is increased. An experiment by Cirillo and Iorio (2004) was run for 4,000 seconds, and considerable ablation of the electrode was observed (Figure 10). In addition, more energy was produced by the reactor at an output/input ratio of 1.2:1.4 (Cirillo and Iorio, 2004).

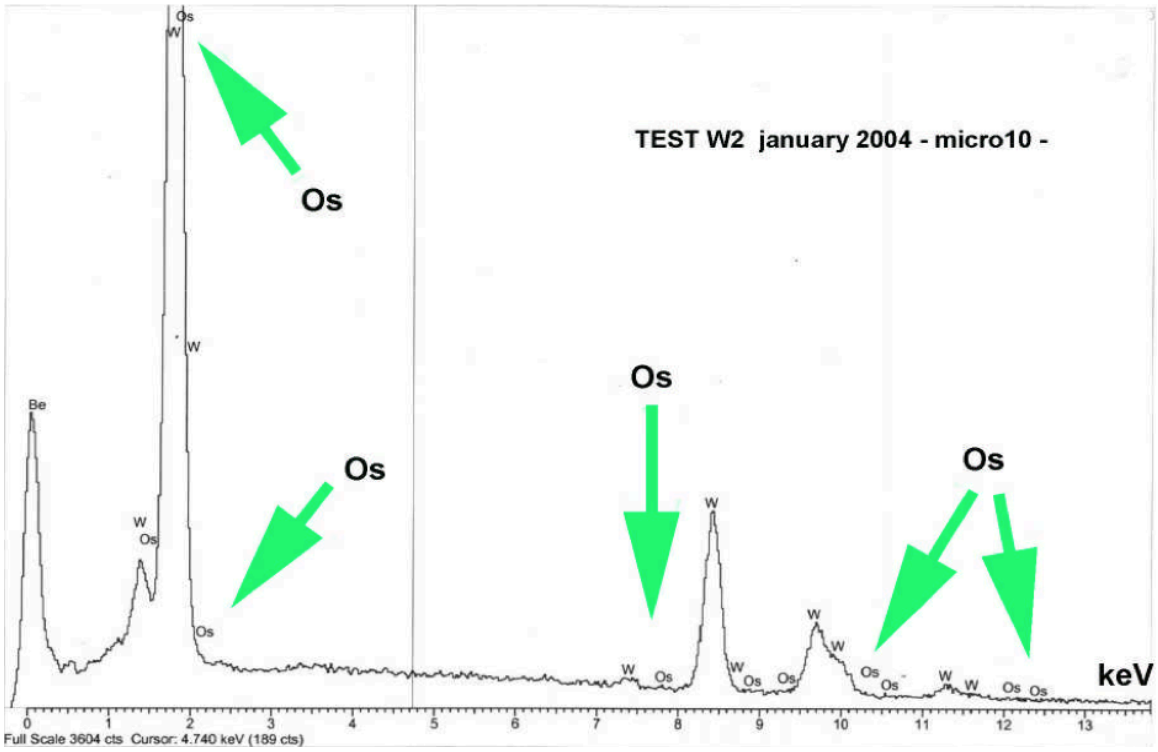

Figure 10. Analysis executed with a scanning electron microscope on an area of the cathode surface after 4,000 seconds of plasma.
Source: Cirillo and Iorio (2004)

The new elements heavier than tungsten detected by energy dispersion X-ray spectroscopy were osmium, rhenium, and gold. Below tungsten were found hafnium, thulium, erbium, ytterbium, and ^{9}Be (Cirillo and Iorio, 2004). This suggests tungsten under MOXY fusion experiences highly excited daughter products with an increased number, and more exotic decay pathways. Tungsten has four stable isotopes. In the experiment by Cirillo and Iorio (2004), ultrapure ordinary water was used, reducing a deuterium-based fusion pathway, which also supports the MOXY hypothesis.

Considering the decay processes observed on the palladium electrode, it was not surprising that hafnium, a possible alpha decay product, was detected on the tungsten. Ytterbium, a potential double alpha decay product of tungsten, was also detected. Double alpha decay might also be imagined as ^{8}Be decay. The significant signature of ^{9}Be is seen in Figure 11. A most interesting finding is the detection of significant amounts of ^{9}Be on the electrode. If an exotic ^{9}Be decay process were possible, it could

account for the detection of thulium and erbium. The hypothesized triple alpha decay could potentially account for erbium.

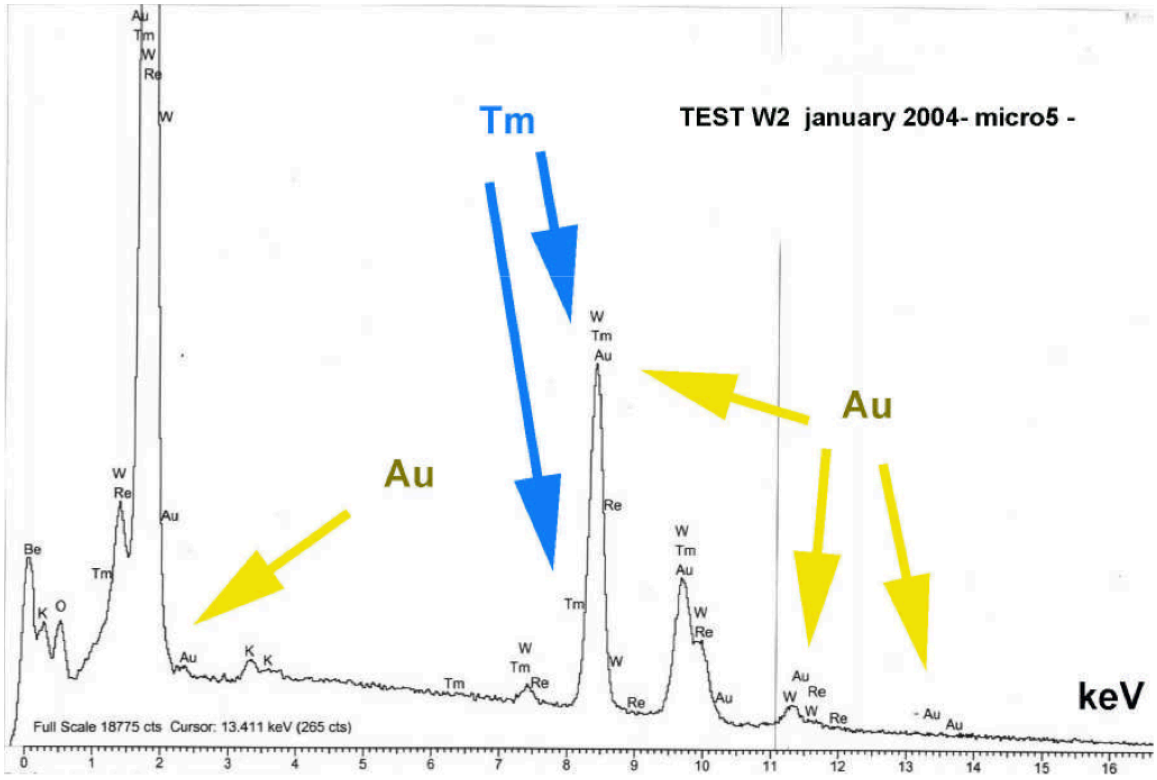

Figure 11. Analysis executed with a scanning electron microscope on an area of the cathode surface after 4,000 seconds of plasma.
Source: Cirillo and Iorio (2004)

Elements expected to be heavier than tungsten by the MOXY model would initially produce highly radioactive isotopes of lead, but with lower than expected binding energies. This may be the reason why lead was not detected. Tungsten is a heavy element, and its proton-to-neutron stability is closer to the ratio of 1:1.5. The single alpha decay pathway of these radioactive lead isotopes would produce mercury, two isotopes of which are potentially stable. It is unlikely that these isotopes would have been detected, because mercury vaporizes between 38°C and 356°C. However, some lead isotopes could possibly decay into gold by exotic ^{9}Be decay or by proton emission from a previous radioisotope, followed by double alpha decay. Gold was detected.

Triple alpha decay would explain the detection of rhenium and osmium. However, given the spectroscopic data, triple alpha decay might be a form of exotic carbon-12 decay. This possibility has the potential to generate a multitude of new decay pathways. It is possible that even more exotic decay pathways are generated with other elements. These highly complex and exotic synthesis/decay pathways are unexplored territory.

It is important to recall the supernova fusion synthesis pathway when considering the results of energy-dispersive X-ray spectroscopy or MOXY. The natural abundance of heavier elements in the solar system comes from supernovas and follows the even–odd rule, where even-numbered (Z) elements are generally 10 times as abundant as their odd-numbered neighbors. Most of the unexpected elements detected were even numbered, and smaller concentrations of odd-numbered elements might exist at lower detection levels. This even–odd rule is shown in the logarithmic chart in Figure 12.

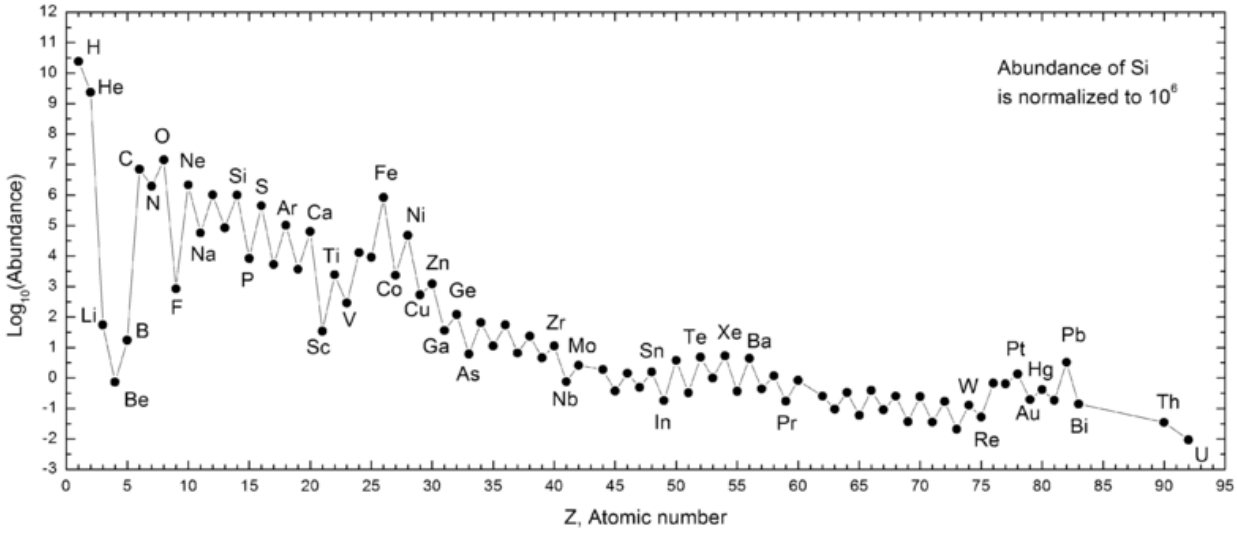

Figure 12. Solar abundance of elements.
Source: Wikimedia Commons user 28bytes, under a CC-BY-SA-3.0, with annotations added by E. Siegel

Potential Remediation of Radioactive Waste by MOXY

Large amounts of spent nuclear fuel have been generated and will remain dangerous for many times longer than human civilization has existed. Serious contamination has also

occurred as a result of numerous radiological incidents. Fortunately, it appears MOXY may be highly effective at reducing the radioisotopes of cesium-137 (^{137}Cs), thorium, and uranium into lighter, nonradioactive elements. With MOXY technology, these wastes can be remediated to reduce the radiological exposure risk to current and future generations.

The experiments of Urutskoev and Filippov (2010) using an explosive electrical discharge between two titanium plates in a uranium salt solution shows a significant reduction in uranium concentrations. The solution consisted of uranyl sulfate in double-distilled water. Double distillation vastly reduces any deuterium in the water.

The electrical energy was delivered in 130 μs pulses at 4.8 kV and 120 kA. The explosive reactor was a sealed stainless steel case, with formed polyethylene holding the foil electrodes and reaction vessel. The reactor was eventually made nonfunctional by the explosive discharges. Testing of the resulting material was accomplished using multiple alpha, beta, and gamma radiation detectors. The results of the experiments are best described directly by Urutskoev and Filippov (2010, p. 232):

> *1) The electric explosion of a titanium foil in an uranyl salt entailed a marked distortion of the initial U isotope distribution in the solution. The "lower" sample… shows depletion in ^{235}U ($R^{lw} = 0.94 \pm 0.01$), while the "upper" sample… shows a more pronounced enrichment ($R^{up} = 1.18 \pm 0.07$).*
> *2) The processes initiated by the electric explosion result in a decrease in the specific concentrations of both U isotopes but the ^{238}U concentration decreases to a larger extent, giving rise to "enrichment effect".*

This selective decrease in the heavier isotope of uranium-238 (^{238}U) with more neutrons is similar to the selective reduction of the heavier isotopes in the titanium electrode, as noted in earlier experiments. Urutskoev and Filippov (2010) also observed a reduction of ^{48}Ti—relative to other, lighter titanium isotopes in the uranyl solution—after the experiment. This uranium reduction is opposite that of natural radioactivity, as ^{235}U has a much shorter half-life than ^{238}U. Both uranium isotopes usually alpha decay initially, and MOXY appears to enhance the alpha decay pathway. No induced fission particles were observed in the samples by the beta and gamma detectors. Hence, a standard model fission pathway was not responsible for the reduced uranium concentrations (Urutskoev and Filippov, 2010).

More interesting results in radioisotope remediation came from the Cincinnati Group, once headed by the late Dr. Robert W. Bass (Mallove, 1997). Bass focused on the reduction of thorium in an apparatus similar to that of Urutskoev and Filippov, although evidently more efficient. The Cincinnati Group (Mallove, 1997) claimed it was able to reduce 0.1 g thorium repeatedly by more than 90% in 1 hour—using only 300 W. The decay products discovered were nonradioactive copper and titanium with unique isotope signatures. The ratio of copper-63 (^{63}Cu) to ^{65}Cu varied from natural abundance by 973%. The several titanium isotopes detected also varied significantly from their natural abundance (Mallove, 1997). MOXY fusion products of a high electron shell level generally have too little binding energy to remain stable, and undergo rapid decay. The observed decay products and lack of expected high-energy emissions tend to support unique MOXY-initiated fission pathways.

This brings to light the interesting possibility that the large binding energy of the actinides might be easily released through the MOXY fusion process—first a MOXY fusion, followed by a rapid fission decay to liberate this binding energy. The process appears aneutronic, and end daughter products are useful monoisotopic nonradioactive elements. This would allow thorium, as well as ^{238}U, to become easily accessed and high-value energy sources.

The Cincinnati Group (Mallove, 1997) also claimed significant reductions in ^{137}Cs and uranium. An examination of possible decay pathways through Bass's method indicates the possible production of highly radioactive, alpha-emitting noble gases and intense X-ray emissions. The Bass apparatus was vented into the atmosphere of the laboratory. The commercial enterprise of the Cincinnati Group is now defunct; it did not survive its founder's untimely passing.

The MOXY process shows great promise in the remediation of heavy radioactive isotopes. As noted earlier, the potential of generating MOXY appears to increase exponentially with elements of greater atomic weights. This allows the actinides, radioactive cesium and strontium, to be remediated efficiently. The technical development of MOXY for nuclear waste remediation may help eliminate this hazard for future generations and awaits further research.

Conclusion

MOXY fusion can help explain the many new elements and excess heat produced by LENRs—the new hydrogen energy phenomenon. This MOXY fusion pathway offers the potential to generate—far into the distant future—safe, clean energy from the vast amounts of deuterium in the oceans. Evidence supporting MOXY fusion comes from numerous sources and with elements of every electron shell level. MOXY provides a conceptual basis for many new fusion synthesis and decay pathways that have yet to be researched. The ability of MOXY to remediate nuclear wastes can help reduce radiological contamination from fission-based nuclear processes and can produce a cleaner world for future generations.

References

Bosch, F., T. Faestermann, J. Friese, F. Heine, P. Kienle, E. Wefers, K. Zeitelhack, K. Beckert, B. Franzke, O. Klepper, C. Kozhuharov, G. Menzel, R. Moshammer, F. Nolden, H. Reich, B. Schlitt, M. Steck, T. Stöhlker, T. Winkler, and K. Takahashi. 1996. Observation of bound-state β–decay of fully ionized 187Re:187Re-187Os cosmochronometry. *Phys. Rev. Lett.* 77(26):5190–5193.

Bulgac, A., M. McNeil Forbes, M.M. Kelley, K.J. Roche, and G. Wlazlowski. 2014. Quantized superfluid vortex ring in the unitary Fermi gas. *Phys. Rev. Lett.* 112. doi: https://doi.org/10.1103/PhysRevLett.112.025301.

Cirillo, D. and V. Iorio. 2004. Transmutation of metal at low energy in a confined plasma in water. Presented at the 11th International Conference on Condensed Matter Nuclear Science, Marseille, France.

Dash, J. and S. Miguet. 1996. Microanalysis of palladium after electrolysis in heavy water. *J. New Energy* 1(1):23–28.

Dash, J. and J. Warner. 2000. Heat produced during the electrolysis of D_2O with titanium cathodes. Presented at ICCF8, SIF Bologna, Italy.

Fleischmann, M. and S. Pons. 1989. Electrochemically induced nuclear fusion of deuterium. *J. Electroanal. Chem.* 261:301–308.

Fox, H. 1997. Charge cluster transmutation. *New Energy News* 5(2):16–20.

Fox, H. 1999. High-density charge and other new-energy devices. *Spirit Ma'at* 2(8): n.p.

Fox, H. and P.G. Baily. 1997. High-density charge clusters and energy conversion results. Presented at the 32nd Intersociety Energy Conversion Engineering Conference, July 27–August 1, Honolulu, HI.

Iwamura, Y., T. Itoh, N. Gotoh, and I. Toyoda. 1996. Correlation between behavior of deuterium in palladium and occurrence of nuclear reactions observed by simultaneous measurement of excess heat and nuclear products. Presented at the Sixth International Conference on Cold Fusion, Progress in New Hydrogen Energy, Lake Toya, Hokkaido, Japan.

Kopecek, R. and J. Dash. 1996. Excess heat and unexpected elements from electrolysis of heavy water with titanium cathodes. *J. New Energy* 1(3):46–54.

Kozima, H., J. Warner, C. Salas Cano, and J. Dash. 2002. TNCF model explanation of cold fusion phenomenon in surface layers of cathode in electrolytic experiments. *J. New Energy* 7(1):81–95.

Krivit, S.B. 2005. How can cold fusion be real, considering it was disproved by several well-respected labs in 1989? Presented at the 12th International Conference on Emerging Nuclear Energy Systems, August 21–26, Brussels, Belgium.

Mallove, E. 1995. Alchemy nightmare: Skeptic finds heavy element transmutation cold fusion experiment! *Infinite Energy* 1(2):30–36.

Mallove, E. 1997. The Cincinnati Group discloses its radioactivity remediation protocol. *Infinite Energy* 13–14:16–29.

Mizuno, T., T. Ohmori, T. Akimoto, and A. Takahashi. 2000. Production of heat during plasma electrolysis in liquid. *Jpn. J. Appl. Phys.* 39:6055–6061.

Nelson, R.A. 1998. The Ohsawa-Kushi transmutations. *J. Borderlands Res.* 54(1):22–25.

Oriana, R.A. and J.C. Fisher. 2003. Energetic charged particles produced in the gas phase by electrolysis. Presented at the 10th International Conference on Cold Fusion, August 21–29, Cambridge, MA.

Passell, T. 1995. Radiation data reported by Wolf at Texas A&M as transmitted by T. Passell. EPRI.

Shoulders, K. and S. Shoulders. 1996. Observations on the role of charge clusters in nuclear cluster reactions. *J. New Energy* 1:111–121.

Shoulders, K. and S. Shoulders. 1999. Charge clusters in action. Bodega, CA (self-published).

Swartz, M.R. 2009. Survey of the observed excess energy and emissions in lattice assisted nuclear reactions. *J. Sci. Exp.* 23(4):419.

Szpak, S., P.A. Mosier-Boss, and J.J. Smith. 1991. On the behavior of Pd deposited in the presence of evolving deuterium. *J. Electroanal. Chem. Interfacial Electrochem*. 302:255–260.

Szpak, S., P.A. Mosier-Boss, C. Young, and F.E. Gordon. 2005. Evidence of nuclear reactions in the Pd lattice. *Naturwissenschaften* 00:1–4.

Urutskoev, L.I. and D.V. Filippov. 2010. Study of the electric explosion of titanium foils in uranium salts. *J. Mod. Phys.* 1:226–235.